Identification of competing ionization processes in the generation of ultrafast electron bunches from cold-atom electron sources

Rory W. Speirs, Andrew J. McCulloch, Ben M. Sparkes, and Robert E. Scholten[*]

School of Physics, The University of Melbourne, Parkville, Victoria 3010, Australia

We make direct measurements of the duration of ultrafast cold-electron bunches produced by photoionization of laser-cooled atoms. We show that the bunch duration can vary by up to six orders of magnitude for relatively small changes in laser wavelength that enhance or inhibit specific photoexcitation pathways and below-threshold tunneling. By selecting a two-color multiphoton excitation process, bunches with durations as low as the measurement resolution limit of 130 ps are measured using a streak technique. Verification that ultrafast cold-electron bunches can be generated by photoionization of cold atoms is an important step towards their application in high-brightness ultrafast electron diffraction and injectors for particle accelerators.

I. INTRODUCTION

High-brightness ultrashort electron bunches are a critical requirement for free-electron lasers [1,2], particle colliders [3], and ultrafast electron diffraction [4–8]. Photocathode sources are the current state of the art in producing bright, ultrafast electron bunches, but ultimately their brightness is limited by the high initial temperature of the electrons produced, typically 10^3–10^4 K [9]. Electron sources based on near-threshold photoionization of laser-cooled atomic gases by ultrafast lasers offer potentially large increases in brightness by greatly reducing the temperature of the electrons generated. These cold-atom electron sources (CAESs) have been shown capable of producing electron bunches with temperatures as low as 10 K [10] and bunch charges up to 80 fC [11], which are approaching values required for the next milestone in nanoimaging: single-shot electron diffraction from micocrystals of large weakly scattering biomolecules [12].

While low temperature and high charge have been demonstrated, the temporal characteristics of electron bunches from a CAES have been largely neglected, even though bunch duration is a critical parameter of sources intended for ultrafast applications [13–15]. It has been implicitly assumed that electron liberation in a CAES takes at most a few picoseconds and the bunch duration is then usually determined by geometrical factors. Time-resolved measurements for single-photon direct photoionization of atoms [16–18] and classical particle tracking simulations of electrons in Stark-shifted Coulomb potentials [19] provide some insight into the processes involved in electron liberation but do not model the many complex electron generation mechanisms active in a CAES. Pulsed electric field ionization of highly excited atoms has been used to create electron bunches from cold atoms with durations of hundreds of picoseconds [20], but offers little prospect of reducing pulse lengths to the ultrafast regime that can be accessed by ultrafast lasers, due to the difficulty of rapidly changing the potential of accelerator electrodes.

Recently, it has been shown that a radio-frequency cavity deflector [21] can resolve the bunch temporal profile of a CAES with picosecond resolution, also allowing identification of the competing excitation and ionization processes. Here we describe direct measurements of the temporal profile of cold-electron bunches produced from a CAES using a simple streak deflection method. We find that photoexcitation to an ionizing state and field ionization of that state can both take significantly longer than the ultrafast excitation laser pulse duration. We show that excitation and ionization are both highly sensitive to small changes in ultrafast laser wavelength and bandwidth, resulting in a variation of electron pulse duration by up to six orders of magnitude. With detailed consideration of these processes, we demonstrate the production of ultrafast cold-electron bunches with duration less than the measurement resolution of 130 ps, consistent with the expected value of a few tens of picoseconds. Such pulses are short enough for compression to 100 fs [22], which will enable the observation of dynamic diffraction on atomically relevant time scales [8].

II. EXPERIMENT

In our experiment, ^{85}Rb atoms are loaded into a mageto-optical trap (MOT) positioned in a static external electric field variable between 1700 and 2600 V cm^{-1}, created by accelerator electrodes separated by 50 mm. The atom cloud is cooled to approximately 100 μK, with a peak density of 10^{10} atoms cm^{-3} and diameter of a few millimeters. After ionization of the trapped atoms, the accelerated electron bunches are focused with a solenoid lens onto a phosphor-coupled microchannel plate detector imaged with a camera. Parallel plate electrodes deflect the beam with a time-varying potential to create a streak on the detector (Fig. 1). The spatial profile of the streak corresponds to the temporal profile of the electron bunches. The potential of the streaking electrodes is ramped using a pair of bipolar push-pull solid-state switches, with a fixed transition time of 10 ns.

To produce an electron bunch, the MOT laser beams were first extinguished to allow the rubidium atoms to decay into the $5S_{1/2}$ ground state and the atoms were then excited via absorption of two or more photons to a field-ionizing state close to the ionization threshold of $E_I = 4.18$ eV. The MOT magnetic coils were also switched off and the field was allowed to decay for 4 ms prior to photoexcitation. We used a dye laser tunable from 460 nm (2.7 eV) to 490 nm
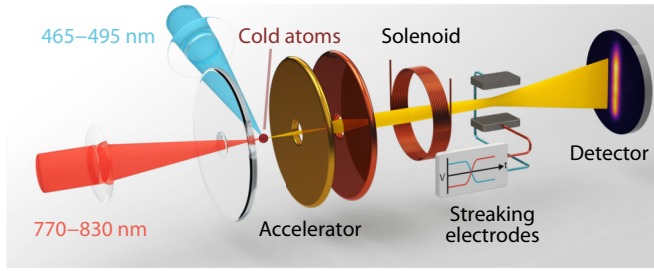
*scholten@unimelb.edu.au

FIG. 1. Electron bunches are produced by photoionization of laser-cooled rubidium gas. The temporal bunch length is determined by applying a time-varying deflection to the bunch while it is drifting and measuring the length of the resulting streak on the detector. Laser-cooling beams and magneto-optic trap coils are not shown; details are in [10].
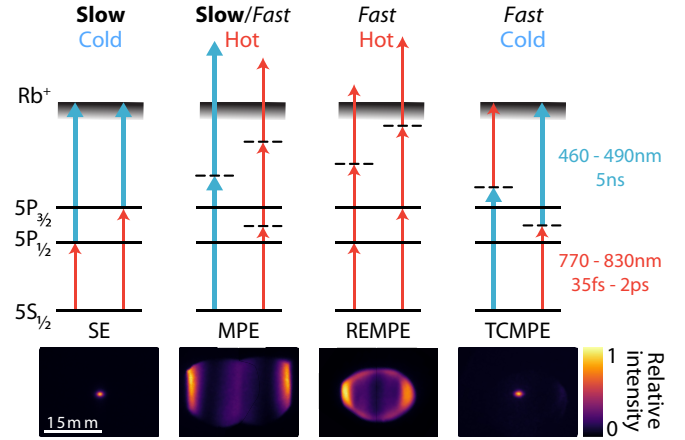

FIG. 2. Simultaneous illumination with two laser pulses can result in several excitation pathways: sequential excitation (SE), multiphoton excitation (MPE), resonance-enhanced multiphoton excitation (REMPE), and two-color multiphoton excitation (TCMPE). Only TCMPE produces electron bunches that are both cold and ultrashort. Virtual states are indicated as dashed lines. The false-color images show transverse momentum distributions of the detected bunches for the associated excitation pathways.

(2.5 eV) to produce blue pulses with a full width at half maximum (FWHM) duration of 5 ns. Red light was provided by either a continuous wave (cw) diode laser tuned to the 780.2 nm $5S_{1/2} \rightarrow 5P_{3/2}$ transition (1.59 eV), pulsed using an acousto-optic modulator with a rise time of a few hundred nanoseconds, or a mode-locked Ti:sapphire amplified pulsed laser. The latter provided wavelengths from 770 to 830 nm and a minimum pulse width of 35 fs. A folded $4f$ pulse shaper [23] selected the central wavelength and bandwidth of the 35-fs pulse with 0.2-nm resolution. The slit selects a wavelength range with a sharp cutoff and if the bandwidth selected is much less than the original 26-nm FWHM, then the spectral density is approximately flat over the selected range. Upon exiting the pulse shaper the pulse intensity profile is given by $I(t) \propto \Delta\omega^2 \mathrm{sinc}^2(\Delta\omega t/2)$, where $\Delta\omega$ is the FWHM frequency range selected. For transform-limited pulses of this form, the time-bandwidth product is given by $\Delta\omega\Delta t = 5.57$, where Δt is the FWHM duration. All laser beams were focused to overlapping waists of approximately 100-μm FWHM within the atomic cloud, with the cw and pulsed red beams illuminating collinearly to electron propagation and the blue beam incident transversely as shown in Fig. 1.

III. EXCITATION PATHWAYS

Atoms can be excited by several different pathways (see Fig. 2), separately or in parallel, with each pathway resulting in different electron bunch temperature and duration. All processes are observed, but each can be isolated by appropriate control of laser wavelength and intensity.

Sequential excitation (SE) [24] uses a single-photon transition from the ground state to an intermediate state and another single-photon transition from the intermediate state to a field-ionizing state. The duration of the excitation process is determined by the duration of the laser pulse driving the transition to the ionizing state, depletion of the intermediate state through that process, or the lifetime of the intermediate state, whichever is shortest.

Even with the relatively-low-energy laser pulses used in our experiments, focusing of the laser beams can easily produce sufficient intensity to cause nonlinear optical transitions. Multiphoton excitation (MPE) [25] occurs when two or more photons are absorbed without the atom transitioning to a real

intermediate state. The transition rate is proportional to the nth power of optical intensity, where n is the number of photons absorbed before the atom reaches its final ionizing state [26]. The lifetimes of intermediate virtual states are very short [27,28], so the excitation period is determined only by the duration of the laser pulse.

Resonance-enhanced multiphoton excitation (REMPE) [25] is a combination of sequential excitation and multiphoton excitation, where m photons are absorbed to excite the atom to a real intermediate state and then a further p photons are absorbed in the transition to the final state. The reduction in the required number of photons for each transition, relative to the number required for a single n-photon transition, can significantly increase the overall transition rate. The excitation duration is limited by the same factors as for sequential and multiphoton excitation.

Two-color multiphoton excitation (TCMPE) [29] is an MPE process where one photon is absorbed from each of two different laser fields. The excitation duration is then determined by the shorter of the two laser pulses.

Cold-electron bunches are produced when the extracted electrons have small excess energy ΔE above the barrier formed by the Stark-shifted Coulomb potential $V = ke/r + Fz$, where r is the distance to the ion core, z is the position in the direction of the external electric field of strength F, k is the Coulomb constant, and e is the elementary charge. The energy of an electron relative to the classical ionization threshold energy is given by

$$\Delta E(F) = -E_I + \sum_{i=1}^{n} \frac{hc}{\lambda_i} + 2\sqrt{ke^3 F}, \qquad (1)$$

where E_I is the field-free ionization energy of the ground-state atom, the middle term is the total energy of the n photons involved in excitation, each with wavelength λ_i,

the third term is the Stark shift of the classical ionization threshold corresponding to the saddle point energy, h is the Planck constant, and c is the speed of light. This assumes a hydrogenlike system, which is an excellent approximation on the condition that $E_I \gg 2\sqrt{ke^3F}$, since at energies near the field-free ionization threshold the shielding effect of the inner electrons has little effect on the energy of the Stark saddle. With our lasers, both SE and TCMPE produce cold-electron bunches with small transverse momentum spread as shown in Fig. 2, but only for TCMPE is the expected excitation duration determined by the ultrafast laser pulse duration.

Directly imaging the unfocused, unstreaked electron bunches after propagation gives a good indication of their temperature. While not technically in the far field, the transverse electron profile imaged on the microchannel plate is approximately equal to the transverse momentum distribution of the constituent electrons scaled for the necessary time of flight and particle mass, convolved with the transverse spatial profile of the bunch at the time of creation, ignoring the magnification due to the accelerator structure. In Fig. 2, the size of the detected bunches generated by both SE and TCMPE processes is dominated by the size of the original bunches, signifying that the election temperature is so low that meaningful values cannot be extracted with this method. The electron temperature can be estimated based on the calculated excess energy and equating energy to temperature using $\Delta E = k_B T$, where k_B is the Boltzmann constant. The SE and TCMPE generated electrons shown in Fig. 2 were both calculated to have a ΔE around 1 meV based on the wavelengths used and field strength of 2140 V cm^{-1}, which corresponds to a temperature of order 10 K. This value is consistent with previous temperature measurements made using the SE process, which was shown to generate electrons with temperature as low as 10 K [10].

The REMPE-generated electrons resulted from the absorption of three photons from the ultrafast laser with wavelength around 780.2 nm, exciting the $5P_{3/2}$ resonance. These electrons had a calculated ΔE of 625 meV, which corresponds to a temperature of 7200 K. Electrons produced via MPE using two blue photons of wavelength 482.1 nm had a calculated ΔE of 1000 meV corresponding to a temperature of 11 600 K. Given the calculated excess energies, the maximum transverse velocity of the MPE electrons is expected to be 1.3 times that of the REMPE electrons. This is supported by the transverse profiles shown in Fig. 2, where the ratio of maximum MPE to REMPE bunch diameters is 1.5. The discrepancy between the expected and calculated diameters is attributed to uncertainties in aligning the composite image for the MPE profile, which was required because the MPE electrons were so hot that any single bunch was partially occluded by apertures in the beamline.

To investigate how the different photoexcitation processes that result in cold electrons affect the duration of generated bunches, electrons were generated under a variety of laser illumination conditions and streaked to determine their duration. Figure 3(a) shows the temporal profile of an electron bunch produced by sequential excitation, using the cw laser to excite atoms to the intermediate state and the pulsed blue laser for excitation to the ionizing state. The bunch duration is 5 ns, mirroring the profile of the blue laser pulse as expected. These
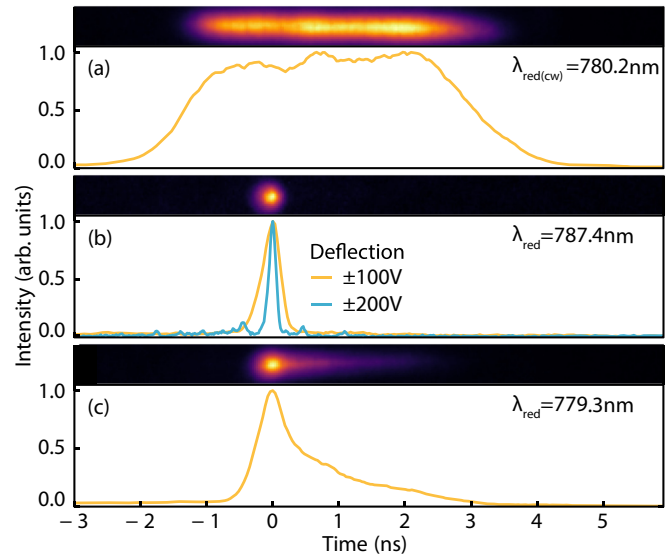

FIG. 3. Electron streak profiles showing pulse broadening by intermediate-state population. (a) Resonant cw excitation. The electron pulse profile mirrors the 5-ns blue laser pulse profile. (b) Far from resonance with intermediate states. TCMPE results in ultrafast bunches (profile in blue produced using higher streaking voltages). (c) Red photons from the ultrafast laser addressing an intermediate state lead to a slow sequential excitation component. The images show false-color detected streaks.

bunches typically contain around 10^5 electrons, with a peak ionization efficiency of greater than 50% [30].

Ultrafast TCMPE was achieved by increasing the intensity of the blue laser pulse and replacing the cw laser beam with a pulse from the ultrafast red laser tuned to 787.4 nm, far from resonance with real intermediate states. The ultrafast laser bandwidth was set to 1 nm and the blue laser was tuned to 482.1 nm, resulting in a small positive ΔE with a 2-meV bandwidth. The measured duration for the resulting electron bunch was 320-ps FWHM as shown in Fig. 3(b), much shorter than the blue laser pulse, thus showing the expected suppression of SE and enhancement of TCMPE in the excitation process.

The actual pulse length of our TCMPE bunches is expected to be much shorter than the 320 ps measured because the temporal resolution of the electron streak is limited by the transverse focal spot size of the detected electron bunch and the achievable deflector slew rate. The focal spot size is fixed by the combination of the bunch transverse emittance, and the numerical aperture and aberrations of the solenoid lens, but temporal resolution can be altered by varying the supply voltages to the deflector electrodes. Doubling the amplitude of the deflector potential, we observed a bunch duration of 130-ps FWHM [Fig. 3(b), blue curve], but again this is limited by the measurement resolution since the image of the streak still appeared circular [as is the case in Fig. 3(b)], indicating that the pulse was so short that the deflection distance was much less than the focal spot size. The deflector potential could not be increased further without inducing electrical breakdown.

The true bunch temporal profile will be given by a convolution of the ultrafast laser pulse profile, the temporal

profile of electron extraction from the ionizing state, and the temporal point spread function due to the spread of electron velocities caused by position-dependent energy imparted by the accelerator. To a first approximation, the actual duration at the streaking electrodes will simply be a sum of the duration of each of these three processes. The ultrafast laser duration is $\Delta t = 1.8$ ps with 1-nm bandwidth centered around 787 nm. Electron extraction time from the excited state is discussed in more detail below, but it is expected to take a few tens of picoseconds for the positive ΔE used here, based on high-resolution streaking experiments [21,31] and classical particle tracking simulations of electrons in Stark-shifted Coulomb potentials [19].

The temporal point spread function (TPSF) represents the change in duration of a hypothetical instantaneously created bunch as it propagates. The bunch spreading is caused by differences in kinetic energy ΔT gained by electrons generated along the length of the ionization region Δz in the accelerator: $\Delta T = eF\Delta z$. The TPSF was calculated assuming constant acceleration in each of the two accelerator regions and ignoring the effects of fringing fields caused by the holes in the electrodes through which the electrons pass.

The field strength in the first acceleration region where the electrons were created was 2140 V cm^{-1} and the mean acceleration distance was 25 mm. The field strength in the second region was 6300 V cm^{-1} with a 10-mm separation between electrodes. Assuming a Δz of 100 μm in the first accelerator region, the TPSF upon exiting the last electrode is 2.1 ps.

The TPSF has a minimum value of 2.6 fs at 153 mm from the last electrode. It is likely that the fringing fields would have some effect on the TPSF at such small time scales, making this value a lower limit. The bunch duration measurement was made at the position of the deflectors, 265 mm after the accelerators, where the calculated TPSF was 1.8 ps. Electron thermal energy, of order 1 meV, is negligible compared to the beam energy spread of 21 eV and so does not contribute to the TPSF. Space charge effects are also negligible since the ultrafast bunches consist of only around 100 electrons.

The true duration of the bunch generated by the TCMPE process is therefore likely dominated by the time it takes for the electrons to escape the ionic cores, which depends on the excitation energy and field strengths as previously mentioned. Using a value of several tens of picoseconds for electron extraction, consistent with values in the literature [19,21,31], the actual electron pulse duration at the deflectors is expected to be less than 50 ps, much shorter than the resolution-limited measurement of 130 ps.

Shifting the central wavelength of the ultrafast laser close to the $5S_{1/2} \rightarrow 5P_{3/2}$ resonance at 780.2 nm results in the generation of electrons by both SE and TCMPE processes, even though the ultrafast laser spectrum does not directly overlap with the resonance. The contribution from both processes is clearly seen from the profile in Fig. 3(c), where there is a fast initial peak but a slow tail of electrons excited from the populated $5P_{3/2}$ state.

The observed pulse broadening shown in Fig. 3(c) is strongly influenced by the wavelength of the ultrafast red laser. Figure 4 shows the pulse duration of electron bunches as the central wavelength of the ultrafast red laser was scanned over
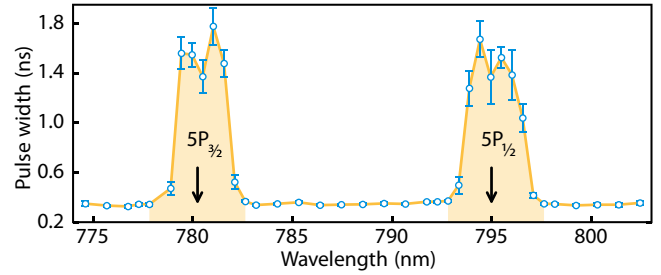

FIG. 4. Measured $1/e$ pulse durations of electron bunches as the ultrafast red laser is scanned over $5P_{3/2}$ and $5P_{1/2}$ resonances. The positions of the resonances are shown with arrows. The shaded area indicates detectable broadening.

both $5P$ resonances. The ultrafast laser bandwidth was set to 0.5 nm and the blue laser wavelength was adjusted such that the total combined photon energy was kept constant, with minimum combined photon energy still resulting in a positive ΔE. Pulse widths of less than 350 ps correspond to resolution-limited durations and the electrons generated in these regions are almost exclusively produced by TCMPE. Pulse widths larger than 350 ps indicate that electrons are being generated after the ultrafast red pulse via SE.

It can be seen that the laser wavelength must be a few nanometers from resonance before broadening by sequential excitation drops below detectable levels, which corresponds to a detuning of around 10^4 natural linewidths. The decrease in bunch duration as the predominant excitation process changes from SE to TCMPE is accompanied by a reduction in total electron yield. Around 10^5 electrons per bunch are created when the ultrafast laser wavelength directly overlaps with a resonance, but only around 100 are produced when exclusively TCMPE electrons are generated.

A complementary excitation scheme that is potentially capable of producing ultrafast bunches with greater electron number uses a slow laser to deliberately populate an intermediate state and an ultrafast laser pulse to further excite the atoms to an ionizing state [32]. The scheme also has the advantage of a reduced likelihood of electron pulse broadening by slow laser excitation to an ionizing state. For example, with rubidium the nearest accessible intermediate state for a pulse of 480-nm (blue) light is the $6P_{1/2}$ level, at a detuning of more than 10^7 natural linewidths [33]. The very large detuning, combined with the lower laser intensities required for the desired single-photon transitions, results in a negligible probability that the excitation process will take longer than the time of the ultrafast laser pulse.

IV. BELOW-THRESHOLD TUNNELING

Regardless of the excitation scheme, rapid excitation of the atom to an ionizing state is not sufficient to generate ultrafast electron bunches: The electron liberation from that state must itself be an ultrafast process. Electrons extracted from Stark-shifted Coulomb potentials have lower transverse momentum spread than would be expected for a given excess energy because the shape of the potential causes anisotropic emission, preferentially directing electrons in the forward direction, along the external electric field. The transverse

momentum spread is therefore reduced and the electron bunches are effectively colder for imaging applications. The coldest electrons, most suitable for high-resolution imaging, have typically been generated by tuning the excitation lasers to, or just below, the ionization threshold. However, our observations show that the duration of electron bunches generated in this way can be increased to an extent that prevents their application to ultrafast imaging.

Below the classical ionization threshold, electrons can escape the atomic potential through tunneling, but the small probability amplitude on the free side of the barrier increases the time it takes to deplete the ionizing state. The sensitivity of tunneling to energy has important consequences for generating ultrafast electron pulses, because the ionization rate of below-threshold Stark states can vary by many orders of magnitude over energy scales that are comparable to the bandwidth of an ultrafast laser pulse.

Above the classical ionization threshold, the probability amplitude on the free side of the barrier is greater and ionization proceeds rapidly. The exact ionization rate depends on which states are excited and the strength of the external field [34], but ionization times in the tens of picoseconds are typical [16–18].

For ultrafast bunch generation with inherently broadband laser pulses, excitation near the classical ionization threshold populates a superposition of Stark states, where electrons from both above and below threshold contribute. Figure 5(a) shows the temporal profile of an electron pulse produced by TCMPE, with the ultrafast red laser tuned so that Stark states were excited with both positive and negative ΔE. A fast initial peak is generated from Stark states with positive ΔE, followed by a very slowly decaying tail from lower-lying states. To study the effects of Stark state lifetime on bunch duration in more detail, the broadband ultrafast red laser was replaced with a narrow-linewidth cw red laser and the pulsed blue laser was used to excite electrons from the $5P_{3/2}$ state. Figure 5(b) shows a resulting streak for $\Delta E = -0.5$ eV, near optimum for imaging because of the resulting low electron temperature. The pulses exhibit long tails with a decay time of 17 μs containing 70% of the total electron charge, corresponding to an increase in bunch length by nearly a factor of 10^6 relative to a bunch generated from purely above-threshold states.

Varying the excess energy ΔE allowed identification of slowly ionizing states as shown in Fig. 5(c). Data in this figure were acquired by varying the electric field strength between 1720 and 2500 V cm^{-1}, using a constant blue laser wavelength of 485.587 nm for excitation to the ionizing state. Variation of the electric field rather than laser wavelength allowed higher-resolution control and avoided laser mode hops.

Electrons produced more than 200 ns after laser excitation were counted by measuring the electrical current to the phosphor screen, while the total electron signal was determined by looking at the integrated light signal generated by the phosphor itself and captured by the camera. Simultaneously capturing both the total and the delayed signal allowed identification of very slowly ionizing excited states. The precise value of ΔE was unknown due to uncertainty in the electric field in the accelerator, so a constant offset was applied to all values of ΔE such that $\Delta E = 0$ corresponded to the onset of states with tunneling times greater than 200 ns. With an excitation energy
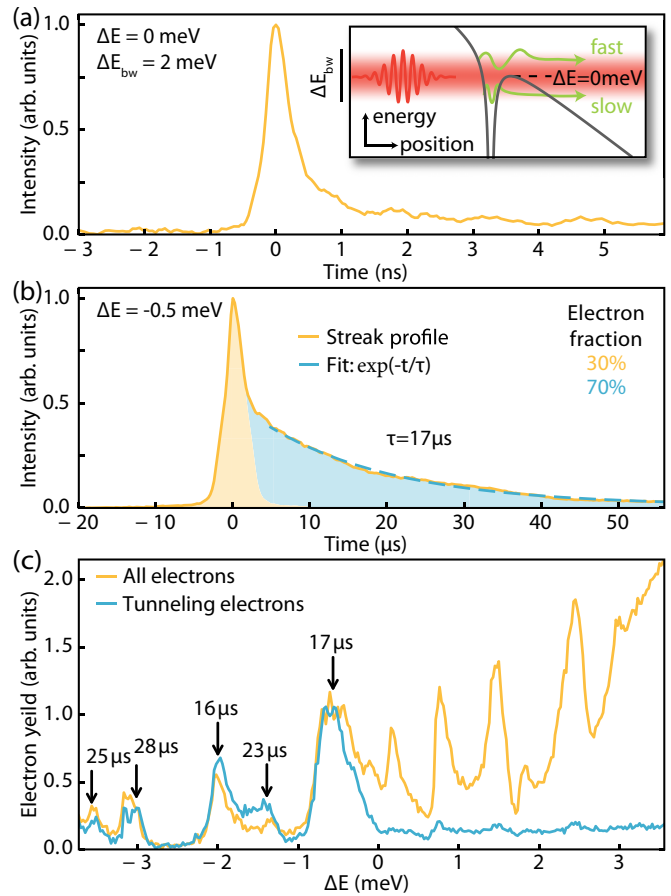

FIG. 5. Slow ionization resulting from tunneling. (a) Temporal profile of the first few nanoseconds of an electron bunch consisting of a fast initial peak due to above-threshold excitation and a slow tail from below-threshold excitation. The ionization process is illustrated in the inset. (b) Complete microsecond-scale profile of an electron bunch generated by below-threshold excitation. (c) Electron yield as a function of excess energy. The yellow line shows the total electron yield and the blue line shows only the yield of electrons detected more than 200 ns after laser excitation. Labels indicate measured pulse decay times at that energy with an uncertainty of ± 2 μs.

below the saddle point energy, the yield of slow electrons rapidly increased. Streak measurements were performed for each discernible state below the threshold, with all showing ionization lifetimes in the tens of microseconds. These ionization time scales are consistent with values reported elsewhere [21] for electrons excited to below threshold energies. Such a drastic and sudden increase in bunch duration shows that it is critically important to avoid coupling to below-threshold states to ensure generation of ultrashort electron bunches.

The slow ionization times observed at lower energies are attributed to tunneling [35] but may also be affected by a combination of other slow internal atomic processes, for example, blackbody-induced transitions to above-threshold states [36] or to below-threshold states with much higher tunneling rates. Regardless of the process, the implications of the slow ionization rates and the requirement to excite to higher energy remain unchanged.

V. CONCLUSION

In summary, we have presented direct measurements of the temporal distribution of electron bunches extracted from cold atomic gases. We have described several distinct processes involved in the excitation and ionization of cold atoms and how each of these processes contributes to the duration of the extracted electron bunches. By identifying the conditions required to ensure that both photoexcitation and electron liberation occur on ultrashort time scales while maintaining favorably low electron temperature, we have verified that it is possible to produce simultaneously ultrafast and cold-electron bunches. Further development of cold-atom electron source technology to increase the bunch charge and ameliorate Coulomb-driven emittance growth [37] could qualitatively change the way ultrafast electron bunches are generated and used, stimulating new developments in ultrafast imaging and particle accelerator design.

[1] J. Fraser and R. Sheffield, IEEE J. Quantum Electron. **23**, 1489 (1987).

[2] P. Emma *et al.*, Nat. Photon. **4**, 641 (2010).

[3] C. Hernandez-Garcia, P. G. O'Shea, and M. L. Stutzman, Phys. Today **61**(2), 44 (2008).

[4] M. Eichberger, N. Erasmus, K. Haupt, G. Kassier, A. von Flotow, J. Demsar, and H. Schwoerer, Appl. Phys. Lett. **102**, 121106 (2013).

[5] B. J. Siwick, J. R. Dwyer, R. E. Jordan, and R. J. D. Miller, Science **302**, 1382 (2003).

[6] V. R. Morrison, R. P. Chatelain, K. L. Tiwari, A. Hendaoui, A. Bruhács, M. Chaker, and B. J. Siwick, Science **346**, 445 (2014).

[7] T. Ishikawa, S. A. Hayes, S. Keskin, G. Corthey, M. Hada, K. Pichugin, A. Marx, J. Hirscht, K. Shionuma, K. Onda, Y. Okimoto, S.-y. Koshihara, T. Yamamoto, H. Cui, M. Nomura, Y. Oshima, M. Abdel-Jawad, R. Kato, and R. J. D. Miller, Science **350**, 1501 (2015).

[8] G. Sciaini and R. J. D. Miller, Rep. Prog. Phys. **74**, 096101 (2011).

[9] B. J. Claessens, S. B. van der Geer, G. Taban, E. J. D. Vredenbregt, and O. J. Luiten, Phys. Rev. Lett. **95**, 164801 (2005).

[10] A. J. McCulloch, D. V. Sheludko, S. D. Saliba, S. C. Bell, M. Junker, K. A. Nugent, and R. E. Scholten, Nat. Phys. **7**, 785 (2011).

[11] R. W. Speirs, C. T. Putkunz, A. J. McCulloch, K. A. Nugent, B. M. Sparkes, and R. E. Scholten, J. Phys. B **48**, 214002 (2015).

[12] T. van Oudheusden, E. F. de Jong, S. B. van der Geer, W. P. E. M. Op't Root, O. J. Luiten, and B. J. Siwick, J. Appl. Phys. **102**, 093501 (2007).

[13] R. P. Chatelain, V. R. Morrison, B. L. M. Klarenaar, and B. J. Siwick, Phys. Rev. Lett. **113**, 235502 (2014).

[14] C. Kealhofer, W. Schneider, D. Ehberger, A. Ryabov, F. Krausz, and P. Baum, Science **352**, 429 (2016).

[15] I. V. Bazarov, B. M. Dunham, Y. Li, X. Liu, D. G. Ouzounov, C. K. Sinclair, F. Hannon, and T. Miyajima, J. Appl. Phys. **103**, 054901 (2008).

[16] B. Broers, J. F. Christian, J. H. Hoogenraad, W. J. van der Zande, H. B. van Linden van den Heuvell, and L. D. Noordam, Phys. Rev. Lett. **71**, 344 (1993).

[17] B. Broers, J. F. Christian, and H. B. van Linden van den Heuvell, Phys. Rev. A **49**, 2498 (1994).

[18] G. M. Lankhuijzen and L. D. Noordham, Phys. Rev. A **52**, 2016 (1995).

[19] W. Engelen, Coherent electron bunches from laser-cooled gases, Ph.D. thesis, Technische Universiteit Eindhoven, 2013.

[20] B. M. Sparkes, D. Murphy, R. J. Taylor, R. W. Speirs, A. J. McCulloch, and R. E. Scholten, Phys. Rev. A **94**, 023404 (2016).

[21] J. Franssen, T. Frankort, E. Vredenbregt, and O. Luiten, Struct. Dyn. **4**, 044010 (2017).

[22] T. van Oudheusden, P. L. E. M. Pasmans, S. B. van der Geer, M. J. de Loos, M. J. van der Wiel, and O. J. Luiten, Phys. Rev. Lett. **105**, 264801 (2010).

[23] A. Monmayrant, S. Weber, and B. Chatel, J. Phys. B **43**, 103001 (2010).

[24] B. Barrett, I. Chan, C. Mok, A. Carew, I. Yavin, A. Kumarakrishnan, S. Cahn, and T. Sleator, Adv. At. Mol. Opt. Phys. **60**, 119 (2011).

[25] K. Kulander, in *Springer Handbook of Atomic, Molecular, and Optical Physics*, edited by G. W. F. Drake (Springer, Berlin, 2006), pp. 1077–1089.

[26] C. J. Joachain, N. J. Kylstra, and R. M. Potvliege, *Atoms in Intense Laser Fields* (Cambridge University Press, Cambridge, 2012).

[27] M. B. Robin, Appl. Opt. **19**, 3941 (1980).

[28] K. D. Belfield, K. J. Schafer, Y. Liu, J. Liu, X. Ren, and E. W. Van Stryland, J. Phys. Org. Chem. **13**, 837 (2000).

[29] M. Dörr, R. M. Potvliege, D. Proulx, and R. Shakeshaft, Phys. Rev. A **44**, 574 (1991).

[30] D. Murphy, R. W. Speirs, D. V. Sheludko, C. T. Putkunz, A. J. McCulloch, B. M. Sparkes, and R. E. Scholten, Nat. Commun. **5**, 4489 (2014).

[31] G. M. Lankhuijzen and L. D. Noordam, Phys. Rev. Lett. **76**, 1784 (1996).

[32] W. J. Engelen, M. A. van der Heijden, D. J. Bakker, E. J. D. Vredenbregt, and O. J. Luiten, Nat. Commun. **4**, 1693 (2013).

[33] M. S. Safronova, C. J. Williams, and C. W. Clark, Phys. Rev. A **69**, 022509 (2004).

[34] L. Y. Baranov, R. Kris, R. D. Levine, and U. Even, J. Chem. Phys. **100**, 186 (1994).

[35] M. G. Littman, M. L. Zimmerman, and D. Kleppner, Phys. Rev. Lett. **37**, 486 (1976).

[36] I. Glukhov, E. Nekipelov, and V. Ovsiannikov, J. Phys. B **43**, 125002 (2010).

[37] D. J. Thompson, D. Murphy, R. W. Speirs, R. M. W. van Bijnen, A. J. McCulloch, R. E. Scholten, and B. M. Sparkes, Phys. Rev. Lett. **117**, 193202 (2016).